1988

Electrochemical Production and Corrosion Testing of Amorphous Ni-P

Jose L. Carbajal
Texas A & M University - College Station

Ralph E. White
University of South Carolina - Columbia, white@cec.sc.edu

Publication Info

Journal of the Electrochemical Society, 1988, pages 2952-2957.

DOI: 10.1149/1.2095468
http://dx.doi.org/10.1149/1.2095468

54. A. R. Denaro, P. A. Owens, and A. Crenshaw, *Eur. Polym. J.*, **4**, 93 (1968).
55. A. R. Denaro, D. A. Owens, and A. Crenshaw, *ibid.*, **5**, 471 (1969).
56. A. M. Mearns, *Thin Solid Films*, **3**, 201 (1969).
57. M. J. Vasile and G. Smolinsky, *This Journal*, **119**, 451 (1972).
58. P. J. Dynes and D. H. Kaelble, *J. Macromol. Sci. Chem.*, **A10**, 535 (1976).
59. J. J. Cuomo, J. M. E. Harper, C. R. Guarnieri, D. S. Lee, L. J. Attanario, J. Angilello, C. T. Wu, and R. H. Hammond, *J. Vac. Sci. Technol.*, **20**, 349 (1982).
60. E. G. Spencer, P. H. Schmidt, D. C. Joy, and F. F. Sansalone, *Appl. Phys. Lett.*, **29**, 118 (1976).

Electrochemical Production and Corrosion Testing of Amorphous Ni-P

Jose L. Carbajal* and Ralph E. White*

Department of Chemical Engineering, Texas A&M University, College Station, Texas 77843

ABSTRACT

Ni-P alloys were prepared by electrodeposition under different conditions on a rotating disk electrode. A variety of alloys were prepared ranging from Ni-15P to Ni-25P. An indirect reduction of species in solution involving several steps appears to be favored over the direct reduction at the electrode based on the low P content in the alloy. Energy dispersion x-ray microanalysis was used to determine composition of the alloy. Transmission electron microscopy and x-ray diffraction corroborated the amorphous nature of the structure. The physical and chemical homogeneity of the metallic glasses produced electrochemically is substantiated by the absence of electrochemical localized attack. Thus, a passivation mechanism is proposed which explains the formation of a broad range passive film in alkaline medium and also explains the narrow range of the passive film in acid and neutral media.

Metal alloys with noncrystalline structure have attracted the attention of many researchers in the last two decades for their distinct properties (1). These include corrosion resistance and interesting mechanical and magnetic properties. These alloys can be produced by a variety of methods including electrodeposition. This method has considerable advantages over most other means of production due to the simplicity of the technique (2, 3).

One of the glassy alloys studied extensively is Ni-P. It is interesting that controversy still exists as to whether its structure is amorphous or microcrystalline (4). This is due to the fact that the bulk metal itself is able to dissolve up to 25% of P without a detectable second phase (5). It is usually accepted now that as the P content increases the grain size decreases. This is consistent with the earlier suggestion by Graham *et al.* (6) that Ni-12P is amorphous. This finding has been substantiated by recent studies of the alloy using extended x-ray absorption fine structures (EXAFS) (7). Despite extensive research on this alloy, there still exists a lack of information about the relationship between the electrodeposition parameters and the alloy composition. A model for this electrodeposition recently reported by this laboratory predicts variations in phosphorus concentrations from zero to 40 atom percent (a/o) (8), and other authors (9) have also reported a wide range of compositions for this alloy. On the other hand, Flechon *et al.* (10) and Vafaei-Makhsoos (11) reported a rather narrow range of alloy compositions for electrodeposited Ni-P. Furthermore, despite the fact that amorphous alloys are known to be corrosion resistant (12-15), thorough investigation of the corrosion behavior of Ni-P in different media does not exist.

The present investigation was undertaken to determine the electrochemical conditions for electrodeposition of amorphous Ni-P alloys. Also, the corrosion behavior of electrodeposited Ni-P was investigated using linear polarization and ac impedance in basic, neutral, and acid media, and these results are compared with those of crystalline nickel.

Experimental

Electrode preparation.—The working electrode used was a rotating disk electrode (RDE) with interchangeable bolt heads exposing an area of 0.458 cm^2 to the solution. Copper and aluminium bolts (99.998% pure from Alfa Ventron) were used. The electrode surface was mechanically polished with successively finer grades of emery paper and alumina powder to 0.05 μm. The electrodes thus obtained were mirror-finished and free from scratches and pits. The RDE was used because of simplicity of the system and its well understood hydrodynamics (16). A rotation speed of 1000 rpm was used in this investigation. A conventional three-compartment cell total volume of 100 ml was used. A platinum counterelectrode separated from the main compartment through a fitted glass and a standard calomel electrode as a reference electrode were also used. All solutions were prepared with analytical-grade reagents and triply distilled water.

Electrodeposition.—A standard plating solution for Ni-P (17) was used in both the galvanostatic and potentiostatic deposition. This solution contained 0.76*M* total metallic nickel as nickel sulfate and nickel chloride and 0.99*M* of phosphorus (0.51*M* phosphoric acid and 0.49*M* phosphorous acid). The solution concentration was varied from 0.2 to 0.8*M* in total nickel content. The nickel and phosphorus content in solution was also varied simultaneously from 0.19 to 0.57*M* to study this effect on the alloy composition. The amount of phosphoric acid was maintained constant at 0.51*M* while phosphorous acid was varied from 0.19 to 0.57*M*. The pH of this solution was kept constant at 1. A fresh plating solution was used in each run. Temperature in the solution was kept at 60°C.

Electrodeposition was carried out galvanostatically (from 100 to 400 mA/cm^2) and potentiostatically (from −1.0 to −1.7V SCE). Potentiodynamic deposition was also carried out at a rate of 0.2 mV/s. All samples prepared contained over 12% of phosphorus. This fact seems to be a precondition to get amorphous alloys (6, 7). Such structure and morphology was confirmed by using transmission electron microscopy (TEM) and x-ray diffraction (XRD), and no further attempts were made to characterize the degree of crystallinity in these alloys. The composition of the alloy was obtained by EDS-SEM (energy dispersion x-ray microanalysis scanning electron microscope), as discussed further below.

Electrochemical measurements.—Solutions of 0.1*M* H_2SO_4, 0.5*M* NaCl, 3% artificial seawater (ASW), and 32% NaOH were used to characterize the corrosion behavior of Ni-P. The acidic solutions were at all times purged with N_2, while the basic and neutral solutions were saturated with oxygen.

The working Ni-P electrodes were initially pretreated cathodically for 3-5 min to clean the surface of oxides developed during sample mounting. Next, they were allowed

* Electrochemical Society Active Member.

to reach steady state at open-circuit potential, which took about 5 min. Polarization within 100 mV from the corrosion potential to obtain the Tafel behavior followed, starting from the negative side. After this, steady state at open-circuit potential was reached and anodic polarization −50 mV from this corrosion potential to 1.5V at a rate of 1 mV/s followed. Measurements of polarization were made using a potentiostat EG&G PAR Model 273 interfaced with a microcomputer. Impedance measurements were carried out using a lock-in amplifier EG&G PAR Model 5301 equipped with a two-channel preamplifier Model 5315.

Analysis of the surface.—Samples of Ni-P obtained at different electrochemical conditions, *i.e.*, galvanostatic and potentiostatic, were analyzed using an EDS-SEM technique. This technique uses a JEOL JSM-35 CF scanning electron microscope in conjunction with Tracor Northern TN-2000 x-ray analysis system. Data was analyzed by a standardless semi-quantitative (SSQ) analysis program which does not require standards for processing electron beam excited x-ray fluorescence spectra. The average analysis errors are about 1% absolute error per element per sample. The primary cause of error is the presence of overlapped peaks in the spectrum which are not unfolded by the SSQ program. Ni and P ratios were obtained at three points on the surface of the RDE, *i.e.*, in the center, in the middle, and in the edge.

Thin films (≈1 μm) of the amorphous material for TEM were deposited on aluminum bolts [preparation for depositing on Al is described in Ref. (18)]. These thin deposits were removed from the Al substrate by scraping with a razor blade. Then, they were dispersed in distilled water by ultrasonication, deposited on a carbon support film 400 mesh hexagonal grid, and dried in room temperature air. A Zeiss 10C transmission electron microscope high resolution with top entry stage and accelerating voltage to 100 kV was used for TEM.

X-ray powder diffraction patterns were obtained using a Seifert Scientag automated powder diffraction unit (PAD II) with Ni-filtered CuKα radiation. Scraps of thin deposits were used directly in this x-ray diffraction analysis.

Results

Electrodeposition.—A plot for the potentiostatic deposition of Ni-P is shown in Fig. 1. Here, the total current including hydrogen evolution and the current after subtraction of the hydrogen evolution are shown as functions of potential; one step is apparent in the curve after hydrogen evolution subtraction. The hydrogen evolution current was measured separately in a blank experiment using a

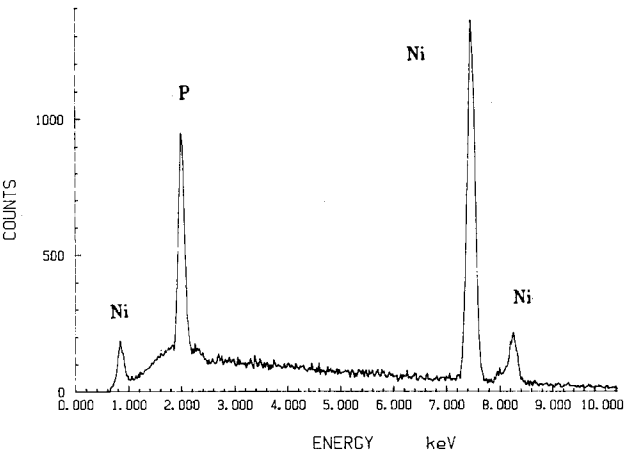

Fig. 2. Typical EDS-SEM spectrum for electrodeposited Ni-P

Ni-P electrode in phosphoric and phosphorous acid solution. A typical EDS spectrum is shown in Fig. 2. The spectrum in Fig. 2 does not show peak overlapping which would decrease the accuracy in the final analysis. Figure 3 shows the composition of the deposited alloy as a function of potential for the standard electroplating solution containing 0.76*M* total metallic nickel and 0.99*M* total phosphorus (0.51*M* phosphoric acid and 0.49*M* phosphorous acid). Variation of the nickel and phosphorus content in the alloy as a function of potential from 76.5 a/o Ni and 23.5 a/o P at −1.1V (SCE) to a 83.5 a/o Ni and 16.5 a/o P at −1.7V (SCE) is observed. Higher P content is obtained at low potentials, and the Ni content increases with cathodic potential. Varying the concentration of nickel in solution from 0.22*M* to 0.76*M* while maintaining the phosphorus concentration fixed at 0.99*M* (0.51*M* phosphoric acid and 0.49*M* phosphorous acid), and at a potential of −1.5V, produced the surface composition variation shown in Fig. 4. An increase of half a mole of nickel in solution produced a 4% increase in Ni content in the alloy, while P decreased about 14%. The compositions of the amorphous deposits obtained varying simultaneously the content of Ni in solution from 0.19*M* to 0.57*M* and the P concentration (phosphorous acid only) from 0.57*M* to 0.19*M* are plotted in Fig. 5 (phosphoric acid fixed 0.5*M*). The amounts of nickel and phosphorus deposited are proportional to their concentrations in the solution.

Alloy microstructure.—TEM results of the alloy did not show the existence of defined rings which are characteris-

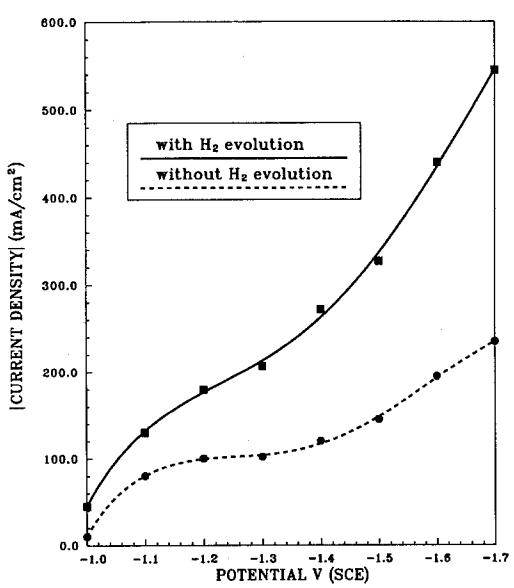

Fig. 1. Current-potential plot for the potentiostatic electrodeposition of Ni-P with hydrogen evolution (——) and without hydrogen evolution (- - -).

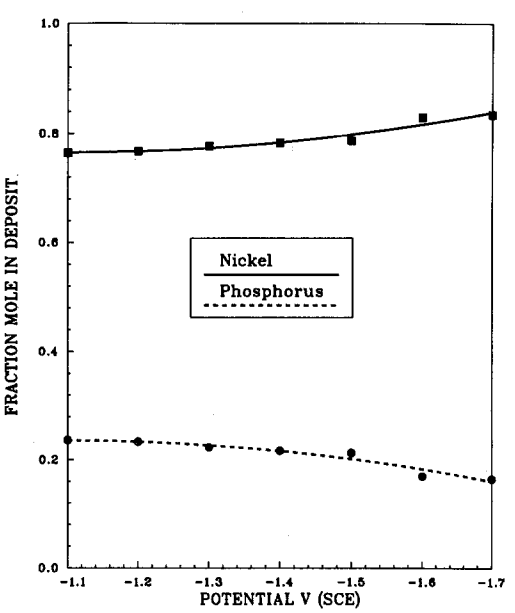

Fig. 3. Dependence of the fractions mole of Ni and P in the electrodeposited alloy on applied potential.

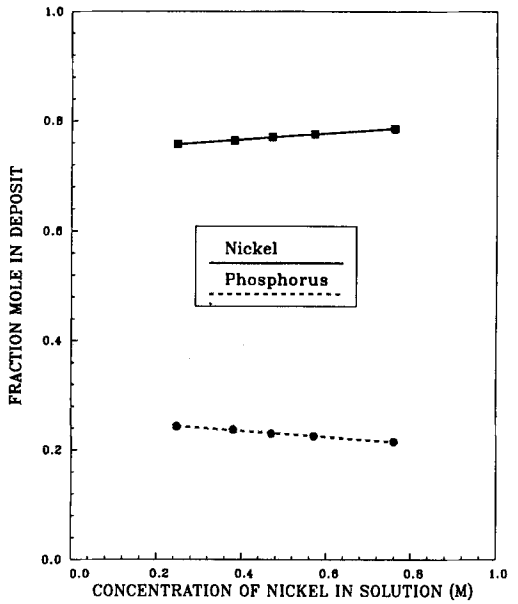

Fig. 4. Dependence of the fraction mole of Ni and P in the deposited alloy on the concentration of Ni in solution at −1.5V and fixed phosphorus (0.99M).

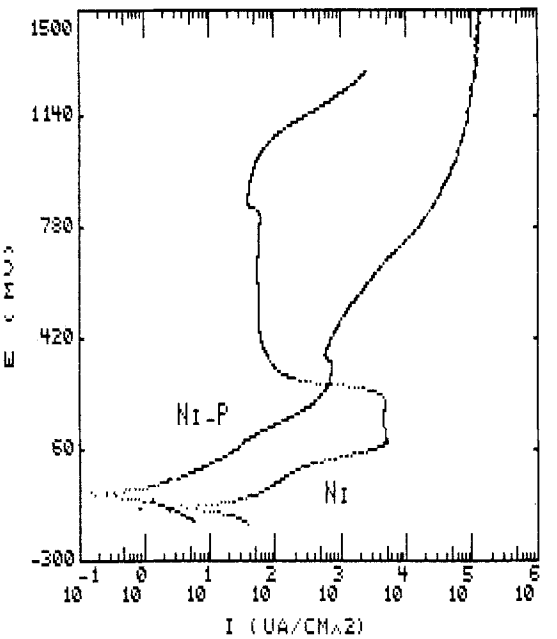

Fig. 6. Anodic polarization behavior of nickel and nickel-phosphorus in 0.1M H_2SO_4 in N_2 atmosphere. Scan rate 1 mV/s.

tic of ordered materials. This, along with the total absence of peaks of the XRD pattern, gives strong indication that the material obtained during the course of this investigation was of amorphous nature. No further attempt was made to characterize the degree of crystallinity of these samples.

Scanning electron micrographs of the Ni-P alloys showed a smooth homogeneous surface. Nickel was deposited for comparison. Pyramidal growth was observed on the nickel deposit.

Corrosion behavior.—A typical anodic polarization plot of Ni-20P alloy in acidic medium (0.1*M* H_2SO_4) compared with crystalline nickel is presented in Fig. 6. The corrosion potential of nickel is slightly more cathodic than Ni-P, and its dissolution rate is faster than that of Ni-P over a range of 300 mV from its corrosion potential. This faster dissolution of nickel provides an active passive region, which is normally a prerequisite for stable passivity. This passivity for nickel extends over a range of about 500 mV. The Ni-20P alloy, on the other hand, continued to dissolve after a formation of a small active passive region. The corrosion behavior of the Ni-20P alloy in 0.5*M* NaCl and 3% ASW is shown in Fig. 7. Passivation is apparent at 0V in this medium. Immediately after a narrow range of passivation, dissolution continues destabilizing such passivation. However, there is not a sharp increase in current which would indicate a breakdown in the oxide film typical of pit formation.

A broader passivation range was obtained for Ni-20P in alkaline medium using a 1*M* solution of NaOH. This is shown in Fig. 8. This passivation extends over a region of about 600 mV with three dissolution peak maxima.

AC impedance results were analyzed assuming a simple electric circuit analog model consisting of a resistance in series with a capacitance and a resistance in parallel. The polarization resistance and the corrosion rate were obtained from these ac impedance data.

Discussion

Electrodeposition.—The faradaic efficiency of the electrodeposition of amorphous Ni-P was determined to be

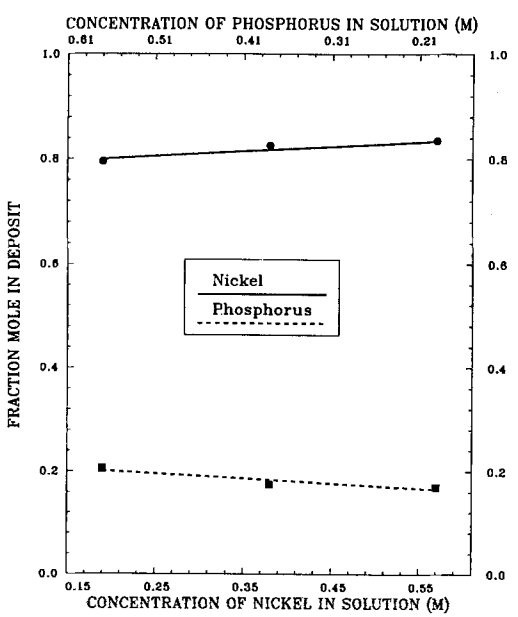

Fig. 5. Dependence of alloy composition on Ni and P concentration in sclution at −1.3V.

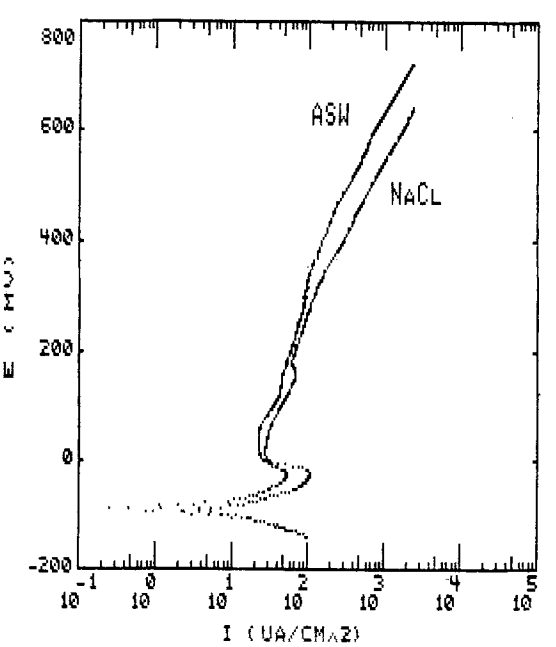

Fig. 7. Anodic behavior of Ni-P in 0.5M NaCl and in ASW in O_2 atmosphere. Scan rate 1 mV/s.

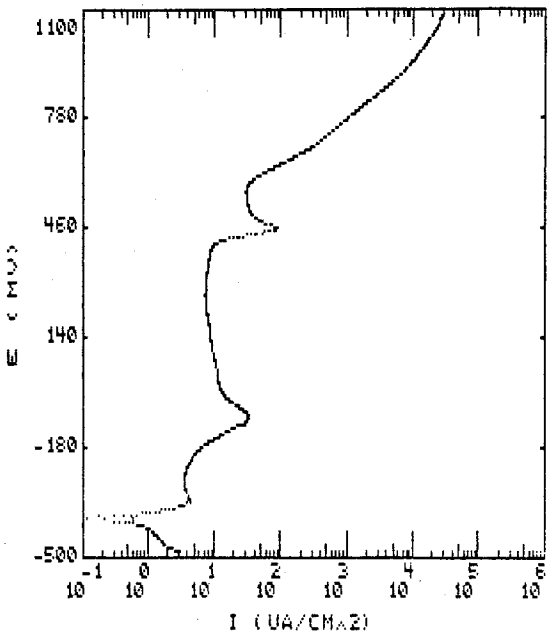

Fig. 8. Anodic polarization curve of Ni-P in 1M NaOH and O_2 atmosphere. Scan rate 1 mV/s.

10 + 2%. This efficiency was determined from samples deposited for 30 min at a polarization potential of −1.5V (SCE). These 30 min periods were used to provide a detectable increase in mass. The main loss of efficiency is due to hydrogen evolution.

This low efficiency can be understood qualitatively by consideration of the processes that occur in electroless and electrolytic plating of Ni-P. In electroless deposition of Ni-P, hypophosphite is employed as the reducing agent. Thus, its concentration directly affects the rate of deposition, and as the plating bath is used up, the hypophosphite ($H_2PO_2^-$) is partly reduced to P but also partly oxidized to phosphite ($H_2PO_3^-$) accompanied by excessive hydrogen evolution in the presence of nickel ions (19)

$$2H_2PO_2^- \rightarrow P + HPO_3^{2-} + H_2O + \frac{1}{2}H_2 \quad [1]$$

$$H_2PO_2^- + H_2O \rightarrow H_2PO_3^- + H_2 \quad [2]$$

In the present electrodeposition, the starting materials are phosphoric, phosphorous acid, and nickel ions. In a direct reduction mechanism (9), phosphorous acid, which is the supplier of P, is partly reduced to hypophosphite at −0.74V (SCE) (20-21). This hypophosphite is further reduced to P at −0.75V (SCE) (20-21) but can also be oxidized by a homogeneous reaction (*c.f.* reaction [2]) at the anode, thereby decreasing the overall efficiency

$$H_2PO_3^- + 2H^+ + 2e \rightarrow H_2PO_2^- + H_2O \quad [3]$$

$$H_2PO_2^- + H^+ + e \rightarrow P + 2H_2O \quad [4]$$

Furthermore, nickel and hydrogen ions can be reduced

$$Ni^{2+} + 2e \rightarrow Ni \quad [5]$$

$$2H^+ + 2e \rightarrow H_2 \quad [6]$$

Here, the reduction to P according to reaction [4], would be the rate-determining step (9).

An indirect mechanism for this electrodeposition has been proposed by Ratzker *et al.* (23)

$$6H^+ + 6e \rightarrow 6H \quad [7]$$

$$H_3PO_3 + 6H \rightarrow PH_3 + 3H_2O \quad [8]$$

$$2PH_3 + 3Ni^{2+} \rightarrow 3Ni + 2P + 6H^+ \quad [9]$$

The direct reduction of hypophosphite ($H_2PO_2^-$) and nickel ions would be expected to produce a codeposition of nickel and phosphorus with high P content in acid medium (up to 51 a/o). On the other hand, the efficiency in the indirect reduction, according to reactions [7-9], with formation of phosphine (PH_3) as an intermediate from nascent hydrogen would be lower. This idea is substantiated by the low percentage of phosphorus in the alloy obtained in this laboratory, which suggests the homogeneous reactions ([1] and [2]) and the nascent hydrogen reaction (*cf.* reaction [7]) control this process.

Phosphoric and phosphorous acid are suppliers of protons. These protons are consumed in the phosphite and hypophosphite reduction (see reactions [3] and [4]), and in the production of hydrogen. Poor dissociation is characteristic of phosphoric acid [pKa = 2.12 (21)] and phosphorous acid [pKa = 2.0 (21)]; thus, there exists a need for protons in solution in order to have efficient reduction of phosphite and hypophosphite.

Figure 1 presents the current-potential plot for the electrodeposition process carried out potentiostatically. This plot includes the total current and the current after the hydrogen evolution current has been subtracted. The plateau in the electrodeposition curve after hydrogen evolution subtraction seems to indicate diffusion limitation in the process. This limitation may be due to Ni^{2+} transport. However, this plateau shows a small slope which would indicate a slow electrodeposition process. This hypothesis can be partly justified by the relative small increase of the Ni mole fraction in the deposit with potential (*cf.* Fig. 3) and with concentration (*cf.* Fig. 4).

Codeposition of Ni and P at all potentials is substantiated by the results of the determination of the alloy composition as a function of potential plotted as shown in Fig. 3. Electrodeposition of Ni-P is greatly reduced by the vigorous hydrogen evolution. The rate of hydrogen evolution according to reaction [6] is about 10 mA/cm^2 at a potential of −1.1V (SCE). With increasing cathodic potential, the production of hydrogen depletes the interface of protons and shifts the *p*H to alkaline at the interface[1]; consequently, hydrogen evolution continues from the reduction of water. However, the reduction of phosphite and hypophosphite according to reactions [3] and [4] require protons which are not available at the interface. This fact will drop the rate of deposition of P as shown in Fig. 3. Flechon *et al.* (9) proposed that the reduction of phosphite and hypophosphite takes place without the need of protons. However, these mechanisms have redox potentials above −2V (SCE). At the most negative electrodeposition potential reached in this work [−1.7V (SCE)], there was no indication that the phosphorus concentration in the alloy would increase with more negative potentials.

At high cathodic potentials, nickel is preferentially deposited over phosphorus as shown in Fig. 3 and 4. This suggests that codeposition of nickel and phosphorus continues though the rate of phosphorus codeposition is slower. An increase in the number of moles of nickel in the solution with a fixed amount of phosphorus increased the amount of nickel in the deposited alloy, as shown in Fig. 4. This is also valid for P, *i.e.*, increase of phosphite in solution increases the content of P in the alloy, as shown in Fig. 5. Galvanostatic deposition of amorphous Ni-P did not show noticeable differences in surface composition within the current density range studied here. The atom percentage present in the surface was 78.4 ± 1.6:21.5 ± 1.6 Ni:P, which roughly accounted for an atom ratio of 4:1.

A qualitative explanation of the structure of the electrodeposited Ni-P can be formulated based on the results presented here and those in the literature. Since nickel electrocrystallization takes place in a face-centered cubic system (fcc), and the codeposition of phosphorus takes place in the octahedron sites, the presence of phosphorus in the nickel crystal lattice would distort its structure, thus breaking the periodicity and producing an amorphous material. When the concentration of P is greater than 12 a/o, mostly amorphous material is obtained (24, 25).

Analysis of the alloy composition in the radial direction within the disk surface was carried out. The composition

[1] Calculation of *p*H changes at the interface at a current density of 10 mA/cm^2 (22), gives a *p*H of 11.5 within a Prandtl boundary layer of 0.001 cm (stirred solution) with an initial *p*H of the solution equal to 1.

in the radial direction did not vary more than 0.1% Nevertheless, these compositions on the disk were averaged over three different points on the surface. Indirect measurement of the deposit thickness was obtained by measuring the copper substrate concentration at three different points on the RDE surface, *i.e.*, at the center of disk, at the middle, and at the edge. A simple calculation made by taking the inverse of the copper concentration at each point (alloy thickness is inversely proportional to copper concentration), provided a method of estimation the relative deposit thickness at these three points. As expected from hydrodynamic calculations on a RDE (26, 27), the deposit thickness from the center of the disk to the edge increased from 1.5 to 2 times relative to the thickness in the center. The thickness of a typical deposit was measured with a profilometer and found to be about 10 μm for the deposition currents and times utilized here.

Corrosion behavior.—It is apparent that in acidic and neutral saline solutions, only a narrow passivation range is obtained on amorphous Ni-P in contrast with the broad passivation range of crystalline nickel, as shown in Fig. 6. However, despite the formation of a passive film on crystalline nickel, pitting may still occur. On the contrary, good pitting resistance was found for the amorphous nickel alloy in a region where the crystalline nickel was pitted.

Tafel extrapolation was used to determine the corrosion potential and current from the intersection of the Tafel lines resulting from the cathodic and anodic polarizations of the electrode. The rate of dissolution of nickel at its corrosion potential is an order of magnitude faster than that of nickel phosphorus. At more anodic potentials, this behavior is reversed (see Fig. 6). In acid medium (0.1*M* H_2SO_4 + N_2), results obtained in this laboratory agree well with results recently published by Diegle *et al.* (15). They used a Ni-P ribbon produced by melt spinning and a solution 0.1*N* sulfuric acid.

The anodic behavior of amorphous Ni-P in acid and neutral saline media shows narrow passivation range, as shown in Fig. 6. Thus, after an active/passive peak maximum at 0.240V, an increase in anodic potential increases the current continuously which indicates dissolution through the passive film is occurring, or there are changes in the oxidation state of the components of the oxide film, or both. These phenomena can be responsible for the brief passivity reached. Analysis of the surface after anodic polarization gave a substantial relative change in the surface composition of up to 25%, showing an enrichment of phosphorus on the surface due to a faster dissolution of nickel. A faster dissolution rate of crystalline nickel over the amorphous nickel phosphorus samples was confirmed during corrosion measurements (Tafel extrapolation and ac impedance).

Structurally, one can argue that the dissolution of crystal planes is kinetically favored compared to the dissolution from amorphous materials due to the existence of several planes of dissolution on the polycrystal (28). In amorphous materials, there is a short-order range which gives great homogeneity to these materials. This property contributes to protect the metal from developing pits during anodization. No localized attack occurred despite the high anodic current in Ni-P during anodic polarization. This can be explained as a high chemical and physical homogeneity of the material prepared electrolytically. This material did not show the formation of pits that nickel developed under the same conditions.

Results of the Ni-P heavy caustic environments as shown in Fig. 8 have not been reported to date. A broad range anodic passivation of Ni-P was obtained in 1*M* and 10*M* NaOH solutions. This passive region extends over 600 mV. Phosphorus is likely oxidized to +3 or to +5 (15, 23). Thus, the three peaks obtained during the anodic polarization of amorphous nickel in caustic media can be assigned to different processes. The first peak closest to the corrosion potential can be said to be a partial oxidation of P to the state +3; the intermediate peak can be associated to a pure nickel dissolution that ends up in its passivation which extends over 600 mV. This passivation is produced by precipitation of nickel hydroxide after reaching its solubility product limit under these conditions. The third peak can be assigned to a change in the oxidation state of phosphorus to the +5 state immediately followed by oxygen evolution, which has a reversible potential of about 0.644V (SCE). Similar behavior was found by Sorensen *et al.* (29) for the oxidation of Cr +3 to +6.

The stable passive film developed on amorphous Ni-P in alkaline solutions may have similar characteristics to that developed on iron in borate buffer solution (30-33). This iron passive film is considered by many authors (30-33) to be an amorphous hydrated hydroxide film. It has been found recently that borate is strongly bonded to the iron surface thus providing great protection to it. Further, it has also been found (34) that this film does not break down in the presence of phosphate ions. One can assume that in alkaline medium, the Ni-P alloy develops similar amorphous hydrated hydroxide film. Also, one can assume that the presence of oxidized P would extend the protection of the surface. Thus, the existence of a passive film on Ni-P is amply justifiable in those terms and is easily substantiated by results presented. Conversely, the presence of protons in the interface during anodic polarization inhibits similar formation on nickel phosphorus alloy at the same time that induces phosphoric acid formation from the oxidized phosphorus. The presence of phosphoric acid at the interface may be the reason for the narrow passivation range shown in Fig. 6. Under these conditions, the interface becomes insensitive to the ions present in solution, as reported by Diegle *et al.* (15).

Conclusions

An efficiency of 10 ± 2% in the electrodeposition process of amorphous Ni-P alloy was obtained. Codeposition of nickel and phosphorus takes place at all potentials. However, the phosphorus rate is higher than that of nickel at low overpotentials; this trend is reversed at high overpotentials. Proton deficiency at the interface may be responsible for rate drop of phosphorus. An indirect reduction mechanism suggested earlier (23) is substantiated by the results obtained. Passivation of Ni-P alloy was obtained in basic, neutral saline, and acid media. Anodic polarization in basic medium shows the existence of three peaks which can be due to changes of oxidation state of phosphorus and nickel. Phosphate formation may be responsible for broad passivation potential in this medium. A small passivation range in acidic and saline neutral media is followed by a continued increase in current with anodic potential. This indicates either dissolution through the passive film or a change of oxidation state of the components or both.

Acknowledgments

The authors are grateful for the support of this project given by the Texas Advance Technology Research Program (TATRP), the Texas A&M University Board of Regents through the Available University Fund (AUF), and Sandia National Laboratories. Thanks are also due to G. Zhang, T. Yeu, and to J. M. Ehrman for their assistance in this work.

REFERENCES

1. R. B. Diegle, *Mater. Eng.*, **96,** 46 (1982).
2. I. deIorio, V. Tagliaferri, and L. Lanotte, *J. Met.*, Nov., 48 (1985).
3. B. G. Bagley and D. Turnbull, *J. Appl. Phys.*, **39,** 12 (1968).
4. E. Vafaei-Makhsoos, E. L. Thomas, and L. E. Toth, *Metall. Trans.*, **9A,** 1449 (1978).
5. Y. S. Tyan and L. E. Toth, *J. Electron. Mater.*, **3,** 791 (1974).
6. A. H. Graham, R. W. Lindsay, and H. J. Read, *This Journal*, **112,** 401 (1965).
7. T. Okamoto and Y. Fukushima, *J. Non-Cryst. Solids*, **61,** 379 (1984).
8. S. Chen, K. M. Yin, and R. E. White, *This Journal*, **135,** 2193 (1988).
9. R. Narayan and M. N. Mungole, *Surf. Tech.*, **24,** 233 (1985).
10. J. Flechon, S. Karkal, and G. Mbemba, *Mater. Chem.*

Phys., **13,** 551 (1985).
11. E. Vafaei-Makhsoos, *J. Appl. Phys.*, **51,** 6366 (1980).
12. A. G. Revesz and J. Kruger, "Passivity of Metals," R. P. Frankenthal and Jerome Kruger, Editors, p. 137, The Electrochemical Society, Princeton, NJ (1978).
13. T. Masumoto and K. Hashimoto, *Anal. Rev. Mater. Sci.*, **8,** 215 (1978).
14. R. M. Latanision, J. C. Turn, Jr., and C. R. Campeau, "Mechanical Behavior of Materials," K. J. Miller and R. F. Smith, Editors, *This Journal*, Pergamon Press, Ltd., Oxford, England (1979).
15. R. B. Diegle, N. R. Sorensen, and G. C. Nelson, *This Journal*, **133,** 1769 (1986).
16. M. H. Rodgers and G. N. Lance, *J. Fluid Mech.*, **7,** 617 (1960).
17. A. Brenner, "Electrodeposition of Alloys," Vol. II, Academic Press, New York (1963).
18. "Canning Handbook of Electroplating," 22nd Ed., W. Canning, Ltd., Gt. Hampton St., Birmingham B186AS (1977).
19. V. K. Gonda, S. Shawki, and H. El-Tawil, *Met. Finish.*, May, 77 (1972).
20. M. Pourbaix, "Atlas of Electrochemical Equilibria in Aqueous Solutions," Pergamon Press, New York (1966).
21. "CRC Handbook of Chemistry and Physics," 63rd ed., CRC Press, Boca Raton, FL (1982).
22. J. O'M. Bockris, J. L. Carbajal, B. R. Scharifker, and K. Chandrasekaran, *This Journal*, **134,** (1987); J. L. Carbajal, Ph.D. Dissertation, Texas A&M University, College Station, TX (1986).
23. M. Ratzker, D. S. Lashmore, and K. W. Pratt, *Plat. Surf. Fin.*, Sept., 74 (1986).
24. P. A. Albert, Z. Kovac, H. R. Lilenthal, T. R. McGuire, and Y. Nakamura, *J. Appl. Phys.*, **38,** 1258 (1967).
25. H. Maeda, *Trans. Nat. Res. Inst. Met.*, **12,** 211 (1970).
26. M. C. H. KcKubre and D. D. Macdonald, *This Journal*, **127,** 632 (1980).
27. J. Newman, *ibid.*, **113,** 1235 (1966).
28. J. O'M. Bockris and G. A. Razumney, "Fundamental Aspects of Electrocrystallization," Plenum Press, New York (1967).
29. N. R. Sorensen, F. J. Hunkeler, and R. M. Latanision, *Corrosion*, **40,** 619 (1984).
30. T. Pou, O. Murphy, V. Young, J. O'M. Bockris, and L. Tongson, *This Journal*, **131,** 1243 (1984).
31. D. Cocke, P. Nilsson, O. Murphy, and J. O'M. Bockris, *Surf. Interf. Anal.*, **4,** 94 (1982).
32. R. Nishimura, K. Kudo, and N. Sato, *Surf. Sci.*, **96,** 413 (1980).
33. N. Sato, K. Kudo, and T. Noda, *Z. Phys. Chem., N. F.*, **98,** 271 (1975).
34. B. R. Scharifker, M. A. Habib, J. L. Carbajal, and J. O'M. Bockris, *Surf. Sci.*, **173,** 97 (1986).

Electrodeposition of Copper-Nickel Alloys from Citrate Solutions on a Rotating Disk Electrode

I. Experimental Results

Ramona Y. Ying*

General Motors Research Laboratories, Physical Chemistry Department, Warren, Michigan 48090-9055

ABSTRACT

Steady-state polarization measurements on stationary and rotating disk electrodes were performed in Cu-Ni-citrate plating baths as well as in single metal ion-citrate solutions. The polarization curves were used to identify the different electrode reactions occurring during the plating process. Five electrochemical reactions were found dominant in different potential regions. They were the reduction of hydrogen ion from the dissociation of hydrogenated citrate ion, oxygen reduction, copper deposition, nickel deposition, and reduction of water. Codeposition of Cu-Ni alloy occurred in a fairly narrow electrode potential region (−1.0 to −1.2V *vs.* SCE), where the effects of the side reactions were relatively small. A Levich analysis of the rotating disk data was used to determine the overall kinetic and mass transport parameters of the Cu-Ni alloy electrodeposition process. Finally, compositional and morphological analyses of the alloy plated at constant potentials were also performed.

Interest in electrodeposition of copper-nickel alloys developed mainly due to the alloy's resemblance to Monel metal, which typically consists of 67% nickel, 30% copper, 1.5% iron, and small amounts of several other elements such as carbon, manganese, and silicon. This alloy has been shown to have superior corrosion properties compared to its parent metals. It is generally believed that nickel promotes the production of a nonporous passive copper oxide film (1-3), which once formed prevents further corrosion. This alloy has been tested in such harsh environments as sea water, mineral acids, organic acids and alkalis (4), and is widely used in marine installations. Other favorable properties of Cu-Ni alloys are high strength, malleability, solderability, and ductility, providing additional incentives to plate the alloy. Beside their metallurgical properties, Cu-Ni alloys have selective catalytic properties as well (5).

Electrodeposition of Cu-Ni alloys dates back to 1912 when Bruni and Amadori (6) plated the alloy from an ammoniacal bath. Brenner's extensive review on alloy electrodeposition (7) summarized much of the literature on Cu-Ni alloy plating up to 1960. Since then, continued interest in plating the alloy persists although no commercial application of the process has been developed. Because the standard electrode potentials of copper and nickel are nearly 600 mV apart, the metal ions are complexed with a ligand in order to codeposit the two metals more readily. Over the years, several complexing agents such as cyanide (8), oxalate (9), tartrate (10), citrate (11-13), pyrophosphate (14, 15), and more recently, glycine (16) and L-asparagine (17) have been tried. Citrate and pyrophosphate plating baths thus far appear to be the most promising ones. The citrate bath was studied here.

Most of the past plating studies on this alloy have been empirical in nature, that is the deposit compositions were measured and plotted as functions of the bath compositions and applied current densities. However, due to the varied experimental conditions, it is difficult to use or improve upon such systems to make them commercially viable. Only general observations can be drawn from these studies. For instance, depending on the deposit composition, the color of the alloy deposit can range from pink to gray to black. Smooth, metallic deposits can be obtained at low applied current densities. Yet a high nickel percentage deposit requires a high current density and a high nickel-to-copper molar ratio in solution as well. Unfortunately, many of the alloy deposits tended to be dark, matted, and powdery, rendering them commercially useless.

The study undertaken here attempts to sort out the discrepancies by studying the plating process under well-

* Electrochemical Society Active Member.